FEMS Microbes, 2024, 5, xtae031
DOI: 10.1093/femsmc/xtae031
Advance access publication date: 3 October 2024
Research Article – Microbes & Disease

Trivalent immunization with metal-binding proteins confers protection against enterococci in a mouse infection model

Ling Ning Lam [1], Angie Sedra[2], Jessica Kajfasz[1], Aym Berges[2], Irene S. Saengpet[1], Grace Adams[1], Jeffery Fairman[2], José A. Lemos[1,*]

[1]Department of Oral Biology, College of Dentistry, University of Florida, Gainesville, FL 32610, United States
[2]Vaxcyte, Inc., San Carlos, CA 94070, United States
*Corresponding author. Department of Oral Biology, College of Dentistry, University of Florida, Dental Science Building, D5-06, 1395 Center Drive, Gainesville, FL 32610, United States. E-mail: jlemos@dental.ufl.edu
Editor: [Kimberly Kline]

Abstract

Enterococcus faecalis is ranked among the top five bacterial pathogens responsible for catheter-associated urinary tract infections, wound infections, secondary root canal infections, and infective endocarditis. Previously, we showed that inactivation of either the manganese- and iron-binding (EfaA) or zinc-binding (AdcA and AdcAII) lipoproteins significantly reduced *E. faecalis* virulence. Here, we explored whether immunization using a multi-valent approach induces protective immunity against systemic enterococcal infections. We found that multi-antigen antisera raised against EfaA, AdcA, and AdcAII displayed similar capacities to initiate neutrophil-mediated opsonization, like their single-antigen counterparts. Further, these antigen-specific antibodies worked synergistically with calprotectin, a divalent host metal chelator, to inhibit the growth of *E. faecalis* in laboratory media as well as in human sera. Using the *Galleria mellonella* invertebrate model and mouse peritonitis model, we showed that passive immunization with multi-antigen antisera conferred robust protection against *E. faecalis* infection, while the protective effects of single antigen antisera were negligible in *G. mellonella*, and negligible-to-moderate in the mouse model. Lastly, active immunization with the 3-antigen (trivalent) cocktail significantly protected mice against either lethal or non-lethal *E. faecalis* infections, with this protection appearing to be far-reaching based on immunization results obtained with contemporary strains of *E. faecalis* and closely related *Enterococcus faecium*.

Keywords: enterococci; multivalent vaccine; immunization; trace metal homeostasis; *Enterococcus faecalis*; nutritional immunity

Introduction

While residents of the gastrointestinal tract, enterococci are major opportunistic pathogens notorious for causing a variety of localized and systemic infections, including but not limited to catheter-associated urinary tract infections (CAUTI) (Flores-Mireles et al. 2015), antibiotic-induced intestinal dysbiosis (Ubeda et al. 2010, Chanderraj et al. 2020), surgical site and diabetes-associated wound infections (Bowler et al. 2001, Gjødsbøl et al. 2006, Dowd et al. 2008), endodontic infections (Alghamdi and Shakir 2020), and infective endocarditis (IE) (Fiore et al. 2019). In healthcare settings, enterococci frequently rank among the top five bacterial pathogens of bloodstream infections, surgical site infections, and CAUTI (Mendes et al. 2018, García-Solache and Rice 2019, Werneburg 2022, Farsi et al. 2023), and is the third most common pathogen of IE (Amat-Santos et al. 2015). While the number of species in the genus *Enterococcus* has substantially increased in the last decade, *E. faecalis* and *E. faecium* continue to be responsible for the overwhelming majority of human infections (Mendes et al. 2016, Weiner et al. 2016, Hornuss et al. 2024). Furthermore, opportunistic enterococcal infections are often difficult to treat due to the notoriously hardy nature of this genus that allows its members to thrive under adverse conditions (Gaca and Lemos 2019) as well as high incidence of multidrug-resistant (MDR) strains (Arias and Murray 2012). Furthermore, enterococcal infections are prevalent and have poorer outcomes in vulnerable (at-risk) populations, including older adults, people with disabilities, and immunocompromised and/or chronically ill individuals (Kristich et al. 2014). For these reasons, the development of novel or improved therapies to treat or prevent enterococcal infections, especially in populations that are more susceptible to these bacteria, is urgently needed.

To date, vaccines remain the most effective and safe therapeutic modality to prevent the occurrence or re-emergence of infectious diseases (Saleh et al. 2021). Since the late 1980s, MDR bacterial infections have been on the rise and have been recognized by the World Health Organization as one of the most serious public health challenges of the next century (Iskandar et al. 2022). Over the years, our ability to treat a range of bacterial infections that were once effectively cured with antibiotics has been severely compromised. Because vaccines can trigger long-term protective immune responses (Forthal 2014), they have the advantage of not only protecting the immunized individual but also of conferring protection within a population that perhaps might decelerate the emergence of MDR bacterial strains (Jansen et al. 2021). Substantial innovations have been made in vaccinology over the past decades (Hajj Hussein et al. 2015), which have prompted attempts to develop vaccines against difficult-to-treat infections caused by MDR bacteria. As of last year, a total of 155 bacterial

Received 4 April 2024; **revised** 13 September 2024; **accepted** 2 October 2024

Table 1. Strains used in this study.

	Strain name	Relevant characteristics[b]	References
***Enterococcus faecalis* laboratory strain**	OG1RF (WT)	Oral isolate, Rif^R, Fus^R	Lab stock
***Enterococcus faecalis* clinical strains**	TX0104 (Cat no. HM 201)	Blood isolate; Van^R	[a]
	TX1322 (Cat no. HM 202)	Fecal isolate; Kan^R	[a]
	MMH594 (Cat no. NR 31975)	Blood isolate; Erm^R, Gen^R	[a]
	V587 (also termed EnGen0242) (Cat no. NR 31979)	Urine isolate; Van^R	[a]
***Enterococcus faecium* clinical strains**	503 (also termed 1 137 055) (Cat no. HM 952)	Unknown	[a]
	EnGen0314 (Cat no. NR 31903)	Fecal isolate	[a]
	EnGen0316 (Cat no. NR 31909)	Fecal isolate	[a]
	EnGen0312 (Cat no. NR 31912)	Fecal isolate; Van^R	[a]
	TX0082 (Cat no. HM 460)	Blood isolate; Amp^R, Erm^R, Kan^R, Van^R	[a]
	ERV99 (Cat no. HM 975)	Peritoneal fluid isolate; Amp^R, Van^R, Gen^R, $Strep^R$	[a]

[a]The following strains were obtained through BEI Resources, NIAID, NIH as part of the Human Microbiome Project.
[b]Resistant to kanamycin (Kan^R), vancomycin (Van^R), erythromycin (Erm^R), gentamycin (Gen^R), ampicillin (Amp^R), streptomycin ($Strep^R$), rifampcin (Rif^R), fusidic acid (Fus^R).

vaccines against MDR pathogens are either in pre-clinical or in clinical phase (Frost et al. 2023). Despite the efforts of a small number of researchers, in particular the laboratory of Johannes Huebner that has explored the potential of selected enterococcal polysaccharides and proteins as vaccine candidates (Kodali et al. 2015, Kalfopoulou and Huebner 2020), there are currently no vaccines against enterococci in either the pre-clinical or clinical phase pipelines (Frost et al. 2023).

The ability to scavenge trace metals such as iron, manganese, and zinc from the host environment is an ubiquitous and essential trait of bacterial pathogens (Palmer and Skaar 2016). Similar to other bacteria (Murdoch and Skaar 2022), our group has shown that *E. faecalis* possesses highly efficient iron (EfaCBA, EitABCD, EmtABC, FeoAB, and FhuDCBG), manganese (EfaCBA, MntH1, and MntH2), and zinc (AdcACB/AdcAII) acquisition systems (Colomer-Winter et al. 2018, Lam et al. 2022). We showed that loss of either the manganese-binding EfaA or both zinc-binding (AdcA and AdcAII) lipoproteins severely impaired *E. faecalis* virulence in a number of animal infection models (Colomer-Winter et al. 2018, Lam et al. 2022). In addition, Huebner and colleagues showed that passive immunization with polyclonal antibodies raised against *E. faecium* PsaAfm and AdcAfm provided broad protection against enterococcal infections (Romero-Saavedra et al. 2015). In these studies, the authors demonstrated that immunization of rabbits with PsaAfm (63% identity to *E. faecalis* EfaA) or AdcAfm (73% identity to *E. faecalis* AdcAII) induced opsonic antibodies that mediate killing of both *E. faecium* and *E. faecalis*. Further, passive transfer of either PsaAfm or AdcAfm antisera reduced bacterial burden in the liver of mice infected with *E. faecium* (Romero-Saavedra et al. 2015). In this report, we have further examined the potential of *E. faecalis* manganese- (EfaA) and zinc-binding (AdcA and AdcAII) proteins in combination, to confer protection against systemic enterococcal infections. Our results indicated that immunization with these proteins generates opsonic antibodies, and that passive immunization with either a 2-antigen (EfaA+AdcAII) or 3-antigen (EfaA+AdcA+AdcAII) antisera conferred protection against *E. faecalis* infection in the *Galleria mellonella* infection model, and to both *E. faecalis* and *E. faecium* in an intraperitoneal (IP) challenge mouse model. Finally, we showed that active immunization with the 3-antigen (trivalent) cocktail provided robust protection against both non-lethal and lethal infections with *E. faecalis* in the peritonitis mouse model. Collectively, our findings reveal that either passive or active immunizations with manganese- and zinc-binding proteins confer stronger protection against enterococcal infections in mice when used in combination rather than alone. To this end, our findings support that EfaA, AdcA, and AdcAII are viable candidates and can serve as the basis for the development of a broadly protective multivalent vaccine. Such a vaccine would be beneficial for patients at heightened risk of developing enterococcal infections, as well as for their caregivers and healthcare professionals.

Materials and methods

Bacterial strains and growth conditions

The bacterial strains used in this study are listed in Table 1. Bacteria were grown in brain heart infusion (BHI) broth (BD Difco, New Jersey, USA) at 37°C under static conditions. For growth kinetic assays, overnight cultures were adjusted to an OD_{600} of 0.25 (~1×10^8 colony-forming units (CFU) ml^{-1}) and inoculated into BHI at 1:50 ratio, with changes in OD_{600} over time recorded in an automated growth reader (Bioscreen c, Oy Growth Curves AB, Helsinki, Finland). Starter cultures for *in vitro* and *in vivo* experiments were prepared from overnight BHI cultures adjusted to an OD_{600} of 0.25 in PBS. Experiments using native hCP or $hCP^{\Delta Mn\text{-}tail}$ (gifts from Walter Chazin, Vanderbilt University, USA) were performed in BHI-CB (BHI supplemented with 50% (v/v) CP buffer (40 mM NaCl, 0.5 mM β-mercapethanol, 1.2 mM $CaCl_2$, 8 mM Tris-HCl, pH 7.5). For growth in human sera supplemented with antigen-specific antibodies, inoculum was prepared from overnight *E. faecalis* cultures adjusted to OD_{600} of 0.5 and inoculated at a ratio of 1:1000 into pooled human serum alone or supplemented with 25 µg ml^{-1} of purified antibodies. Heat-inactivated antibodies were prepared by incubation at 65°C for 1 hour. For *E. faecalis* OG1RF CFU determination, serially diluted aliquots were plated on BHI agar supplemented with 200 µg ml^{-1} rifampicin and 10 µg ml^{-1} fusidic acid. For CFU determination of other enterococci, plain BHI agar was used instead. Chemical and biological reagents were purchased from Sigma–Aldrich (St. Louis, MO, USA) unless stated otherwise.

Bioinformatic analysis of EfaA, AdcA, and AdcAII

Amino acid sequence alignment of *E. faecalis* OG1RF AdcA and AdcAII was performed as previously described (Lam et

Table 2. Nucleotide consensus in sequences of clinical isolates.

Strain	BEI catalog no.	BioProject ID	Sequence identity %*	Contigs accession ID
***Enterococcus faecalis* TX0104**	HM-201	30623	EfaA (84, 99.68); AdcA (98.95); AdcAII (98.83)	ACGL01000034.1, ACGL01000223.1 ACGL01000063.1 ACGL01000023.1
***Enterococcus faecalis* TX1322**	HM-202	31461	EfaA (99.57, 68.24); AdcA (99.37); AdcAII (98.96)	ACGM01000011.1, ACGM01000048.1 ACGM01000066.1 ACGM01000099.1
***Enterococcus faecalis* MMH594**	NR-31975	89033	EfaA (99.68, 68.24); AdcA (99.37); AdcAII (98.96)	AJDZ01000011.1, AJDZ01000008.1 AJDZ01000002.1 AJDZ01000018.1
***Enterococcus faecalis* V587**	NR-31979	88873	EfaA (99.68, 68.24); AdcA (99.37); AdcAII (98.96)	AJBB01000014.1, AJBB01000011.1 AJBB01000022.1 AJBB01000021.1
***Enterococcus faecium* TX0082**	HM-460	47193	EfaA (68.88, 67.75); AdcA (64.97, 68.05); AdcAII (68.95, 71.06)	AEBU01000015.1, AEBU01000077.1 AEBU01000046.1, AEBU01000080.1 AEBU01000125.1, AEBU01000127.1
***Enterococcus faecium* 503**	HM-952	81995	EfaA (68.88, 68.49); AdcA (68.05, 64.97); AdcAII (70.84)	AMBN01000022.1, AMBN01000008.1 AMBN01000132.1, AMBN01000191.1 AMBN01000008.1
***Enterococcus faecium* ERV99**	HM-975	82043	EfaA (68.88); AdcA (68.05); AdcAII (66.09)	AMAQ01000181.1 AMAQ01000176.1 AMAQ01000009.1
***Enterococcus faecium* EnGen0314**	NR-31903	89027	EfaA (68.88, 68.49); AdcA (68.05, 64.97); AdcAII (70.84)	AJDX01000051.1, AJDX01000015.1 AJDX01000016.1, AJDX01000029.1 AJDX01000015.1
***Enterococcus faecium* EnGen0312**	NR-31912	89027	EfaA (68.88, 68.49); AdcA (68.05, 64.97); AdcAII (70.84)	AJDX01000051.1, AJDX01000015.1 AJDX01000016.1, AJDX01000029.1 AJDX01000015.1
***Enterococcus faecium* EnGen0316**	NR-31909	89017	EfaA (68.88, 68.49); AdcA (64.97, 68.05); AdcAII (70.84)	AJDS01000014.1, AJDS01000027.1 AJDS01000013.1, AJDS01000029.1 AJDS01000027.1

*Compared to *E. faecalis* OG1RF protein sequences.

al. 2022). To generate phylogenetic trees, amino acid sequences from EfaA, AdcA, and AdcAII proteins of *E. faecalis* OG1RF (EfaA; WP_002356954.1, AdcA; WP_002367576.1, AdcAII; WP_002392710.1) were queried against genomes of *E. faecalis* and *E. faecium* available in the Bacterial and Viral Bioinformatics Resource Center (BV-BRC) database. Among the 4539 *E. faecalis* and 7555 *E. faecium* genome sequences available in the BV-BRC repository, 154 *E. faecalis* and 206 *E. faecium* genomes were selected for comparison based on the following criteria provided by BV-BRC: (i) complete genome, (ii) good quality genome, and (iii) isolated from humans. In consideration of potential orthologs and/or homologs of EfaA, AdcA, and AdcAII, and the limitation of the BV-BRC server in generating large phylogenetic maps, 19 genomes were randomly selected as representative strains isolated from different countries and aligned with *E. faecalis* OG1RF as the reference genome to generate cladogram displays of protein phylogeny. Phylogenetic trees generated were then edited using the Interactive Tree of Life (iTOL) version 5 online software. To identify nucleotide conservation among clinical *E. faecalis* and *E. faecium* isolates obtained from NIH BEI Resources Repository, shotgun sequencing-derived scaffolds of each strain were queried (Table 2) against nucleotide sequences of *efaA* (*OG1RF_RS08610*), *adcA* (*OG1RF_RS00260*), and *adcAII* (*OG1RF_RS12625*) that were obtained from BioCyc genome database.

Construction, expression, and purification of recombinant proteins

Protein expression using Xpress cell free™ protein synthesis (CFPS) (XpressCF+™) platform was performed as previously described with minor modifications (Zawada et al. 2011). Briefly, codon-optimized sequences were synthesized and sub-cloned with an N-terminal methionine into a proprietary vector at ATUM (Menlo Park, CA, USA). Each protein of interest contained an N-terminal histidine-6 tag followed by a TEV protease [ENLYFQG] cleavage site. For titer estimates, microscale cell-free protein synthesis reactions were performed in the presence of radiolabeled ^{14}C-leucine (GE Life Sciences, Piscataway, NJ, USA), of which the incorporation allowed accurate assessment of total protein, including the soluble fraction counterpart in the reaction mixture. Microscale expression test reactions were performed in 100 µl of supermix containing 2% ^{14}C-labeled leucine, plasmid DNA for each polypeptide construct, cell-free *E. coli* extract, T7 polymerase, and water. The complete cell-free reaction supernatant was blotted onto an anion exchange filter membrane, extensively washed to remove unbound material, and heat-dried for 30 min. Finally, the filter membrane was evenly coated with scintillation fluid, air dried, and the counts recorded to estimate the total and soluble yield of the expressed proteins. Next, small-scale protein expression was performed as previously described (Knapp et al. 2007) with minor modifications. Cell-free extracts were incubated with 50 µM iodoacetamide for 30 min at room temperature, and then added to a reaction mix containing 30% (v/v) iodoacetamide-treated extract with 8 mM magnesium glutamate, 10 mM ammonium glutamate, 130 mM potassium glutamate, 35 mM sodium pyruvate, 1.2 mM AMP, 0.86 mM each of GMP, UMP, and CMP, 2 mM of each amino acids (except tyrosine, at 1 mM), 4 mM sodium oxalate, 1 mM putrescine, 1.5 mM spermidine, 15 mM potassium phosphate, 100 nM T7 RNAP, 2–10 µg ml^{-1} plasmid DNA

template, 1–10 µM *E. coli* DsbC. Reduced (GSH) and oxidized (GSSG) glutathione were added to a total concentration of 5 mM. The initial redox potential was calculated using the Nernst equation with E0 = 205 mV as the standard potential of the GSH/GSSG couple at 30°C and pH 7. Proteins produced at the larger scale were then plated evenly in 20 cm Petri dishes, forming a thin layer at the bottom, and the plates incubated at 25°C for 14-16 hours. The pool was harvested the next day at 7500 × g for 35 min, then the supernatant was collected, and the salt content was adjusted to 50 mM Tris pH 8, 150 mM NaCl, and 10 mM imidazole, prior to being subjected to a 0.22 µM filtration. To purify the polypeptide antigens, Ni-beads were used to bind the His-tagged protein. Briefly, 5 ml of HisTrap excel columns were equilibrated in Buffer A (50 mM Tris pH 8, 150 mM NaCl, and 10 mM imidazole), washed once in Buffer A, then Buffer A2 (Buffer A + 0.05% Triton X-100) for endotoxin removal, and followed by another wash in Buffer A to remove the detergent. The polypeptide antigens were eluted using a Buffer B gradient (50 mM Tris pH 8, 150 mM NaCl, and 300 mM imidazole). The fractions corresponding to the elution peak were pooled, and purified proteins cleaved using a ratio of 1:10 TEV protease to protein. Dialysis was performed overnight in 1x TBS. The samples were retrieved and passed over 1 ml HisTrap using 1X TBS as Buffer A, with 300 mM imidazole. The flow-through was collected and concentrated using a 10 kDa cut-off Amicon filter. Flow-through, washed fractions, and eluted fractions were run on sodium dodecyl-sulfate polyacrylamide gel electrophoresis (SDS-PAGE). Gels were stained with Coomassie Blue for size, purity, and TeV cleavage confirmation, and then readout was captured using a Syngene G-box gel imager. The endotoxin level was tested using Charles River Endosafe Nexgen-PTS150 Endotoxin detection system. Aliquots of purified polypeptide antigen were prepared, labeled, and stored at −80°C for future use.

Multi-angle light scattering analysis

SEC Multi-angle light scattering (MALS)-UV-RI was performed with an Agilent HPLC 1100 degasser, temperature-controlled autosampler (4°C), column compartment (25°C), and UV-VIS diode array detector (Agilent, Santa Clara, CA, USA) in line with a DAWN-HELEOS multi-angle laser light scattering detector and Optilab T-rEX differential refractive interferometer (Wyatt Technology, Santa Barbara, CA, USA) coupled to three TOSOH columns in series: TSKgel Guard PWXL 6.0 mm ID 4.0 cm long, 12 mm particle; TOSOH TSKgel 6000 PWXL 7.8 mm ID × 30 cm long, 13 mm particle; and a TSKgel 3000 PWXL 7.8 mm ID 30 cm long, 7 mm particle. A mobile phase consisting of 0.2 mm filtered 1X PBS with 5% (v/v) acetonitrile was used at a 0.5 ml min^{-1} flow rate and 50-100 mg sample injected for analysis. Agilent Open Lab software was used to control the HPLC, and Wyatt Astra 7 software was used for data collection and analysis of molecular weight of purified recombinant proteins.

Antisera and purified polyclonal antibodies preparation

Recombinant AdcA, AdcAII, and EfaA were sent to YenZym Antibodies (Brisbane, CA, USA) to raise rabbit polyclonal antisera. Polyclonal antisera were produced either from single-antigen immunization (AdcA, AdcAII, or EfaA only) or multi-antigen immunization (EfaA + AdcAII, or EfaA + AdcA + AdcAII). Antisera raised from rabbits immunized with alum (adjuvant/vehicle control) were used as controls for downstream experiments. Immunizations were performed via subcutaneous injection of 50 µg antigen in an accelerated 28-day (single antigen; 1 rabbit per group) protocol, or 10 µg antigen in a 77-day (multi-antigen; 3 rabbits per group) standard immunization protocol. Pre-bleeds, production bleeds, and terminal bleeds were obtained and stored at −20°C for future use. A portion of the terminal bleeds from the rabbits immunized with EfaA, AdcA, and AdcAII, respectively, were used to obtain affinity-purified antigen-specific antibodies following YenZym standard protocols.

Measurement of antigen-specific IgG titers in rabbit immune sera

Measurement of IgG titers was performed as previously described (Romero-Saavedra et al. 2015) with minor modifications. Total rabbit IgG concentration in each serum sample was normalized to 2 mg IgG ml^{-1} using the Easy-Titer Rabbit IgG Assay kit (Thermo Scientific, Waltham, MA, USA). Immulon 4 HBX 96-well plates (Thermo Scientific, Waltham, MA, USA) were coated either with 1 µg antigen or with 0.5 µg *S. aureus* LTA (Sigma–Aldrich) in 0.2 M carbonate-bicarbonate coating buffer, pH 9.6. Plates were incubated overnight at 4°C, washed three times with PBS containing 0.05% Tween-20 (PBS-T), and blocked with 3% bovine serum albumin (BSA)-PBS-T at 37°C for 2 hours. After incubation, plates were washed three times with PBS-T, and sera were plated in two-fold serial dilutions and incubated for 1 hour at 37°C. Plates were washed again three times with PBS-T and alkaline-phosphatase-conjugated goat anti-rabbit IgG (Sigma) diluted 1:1000 used as a secondary antibody. After 60 mins of incubation at room temperature, plates were washed three times with PBS-T, and then 100 ul of 1-step PNPP (p-nitrophenyl phosphate) (Sigma) was added to each well and followed by incubation at room temperature for 20 mins. After that, 50 µl of 2 N sodium hydroxide was added to stop the reaction and the absorbance was measured at 405 nm on a Tecan Infinite 200 PRO (Tecan Group Ltd, Morrisville, NC, USA).

Isolation of pooled human serum and neutrophils

Whole blood and buffy coats were obtained from LifeSouth Community Blood Centers (Gainesville, FL, USA) for isolation of human serum and neutrophils, respectively. This procedure was approved and performed in compliance with the University of Florida Institutional Review Board (IRB) Study #IRB202100899. For isolation of pooled human serum, whole blood from 15 donors (type O^+) was pooled, left to stand at room temperature for 30 mins, and centrifuged at 2000 rpm for 10 mins. The resulting serum supernatants were pooled, aliquoted, and stored at −80°C for future use. Isolation of human neutrophils was performed as previously described with minor modifications (Kremserova and Nauseef 2020). Briefly, buffy coats from 7 to 8 donors were pooled and processed on the day of each experiment. An equal volume of dextran-heparin buffer (3% (wt/v) Dextran-500, 0.00568% (wt/v) of heparin, 0.9% NaCl) was added to each donor's buffy coat and incubated at 37°C for 1 hour. After incubation, the leukocyte-rich/erythrocyte-poor supernatant was transferred to a new tube. For each donor, leukocyte pellet was collected by centrifugation at 500 g for 10 mins at 4°C and then pooled together in 30 ml of dextran-heparin buffer. Pooled leukocyte suspension was underlaid with 10 ml of Histopaque 1077 (density, 1.077 g ml^{-1}) and centrifuged at 400 *g* for 40 min at room temperature to isolate the granulocytes and any remaining erythrocytes (PMN-erythrocyte layer). Supernatant above this layer was discarded and PMN-erythrocyte cell pellet suspended in 1% (wt/vol) ammonium chloride for 2–3 mins for hypotonic lysis of remaining erythrocytes. Isolation of neutrophils and complete lysis of erythrocytes was achieved by repeating

hypotonic lysis step and centrifugation at 400 *g* for 5 mins at 20°C. Counting of trypan blue-stained cells using a hemocytometer was performed to determine number of live neutrophils.

Neutrophil-mediated opsonophagocytic assay

In vitro opsonophagocytic assays were performed as previously described with minor modifications (Romero-Saavedra et al. 2015). Briefly, four components were added into Roswell Park Memorial Institute (RPMI) medium (Thermo Scientific, Waltham, MA, USA) supplemented with 15% (v/v) inactivated fetal bovine albumin (Gibco, Waltham, MA, USA): (a) rabbit complement (Rockland, Bedford, PA, USA; added at a ratio of 1:10), (b) the different rabbit antisera (added at a ratio of 1:10), (c) polymorphonuclear neutrophils (PMNs) freshly prepared from pooled buffy coats ($\sim 1 \times 10^6$ cells ml^{-1}), and (d) overnight-grown bacteria normalized to OD_{600} 0.025 ($\sim 1 \times 10^7$ CFU ml^{-1}). All opsonophagocytic assays were performed using a multiplicity of infection (MOI) of 1:10 (neutrophil to bacteria ratio) in a 24-well microtiter plate format. Pre-absorption of bacterial cells to the rabbit antisera was performed for 1 hour at 4°C prior to addition of neutrophils. After adding all components, the microtiter plate was incubated in a shaking incubator at 50 rpm at 37°C for 90 mins. In experiments that require sonication of cells after incubation, samples were sonicated in an ultrasonic water bath using low-intensity setting as previously described (Joyce et al. 2003) (Fisher Scientific, Waltham, MA, USA) for 5 mins, then vortex at maximum speed for 30 secs prior to plating. After incubation, the percentage of neutrophil-mediated killing was calculated by determining CFU of bacteria in the wells that have rabbit antisera compared to those that do not. For each sample, a plot of OD value against the antibody dilution [Log_{10}(antibody dilution)] was used to calculate the intercept with the specified cutoff value of each test, and the extrapolated inverse value was used to generate the end point titer. For inhibition studies, rabbit antisera were first incubated with purified proteins of interest for 1 hour at 4°C prior to addition of all other components. BSA (100 µg ml^{-1}) was used as the protein control. The percentage of inhibition of opsonophagocytic killing was compared to controls without inhibitory proteins.

SDS-PAGE and immunoblot analyses

Samples were prepared for immunoblotting (Nielsen et al. 2013) with minor modifications. Cell pellets were collected by centrifugation, suspended in SDS sample buffer (60 mM Tris, pH 6.8, 10% glycerol, 5% SDS), and then boiled at 100°C for 15 mins. Protein extracts were normalized by protein content using the bicinchoninic acid (BCA) assay kit (Pierce™, Appleton, Wisconsin, USA), and resuspended in 2X SDS sample buffer with 2.5% beta-mercaptoethanol and 0.1 M dithiothreitol (DTT) prior to loading onto 12% separating tris-glycine gel. Immunoblotting was performed using wet transfer to PVDF membranes in Tris-glycine transfer buffer at 100 V for 90 mins at 4°C. After the transfer was complete, the PVDF membrane was soaked overnight in blocking buffer (PBS, 0.05% Tween-20, 3% BSA) at 4°C with constant agitation. The next day, the membrane was washed thrice with washing buffer (PBS-T) followed by 1 hour incubation with rabbit antisera (1:1000) in blocking buffer, and 1 hour incubation with secondary goat anti-rabbit antibody (Invitrogen, Carlsbad, CA, USA) (1:5000) with washes before and after each incubation. Proteins were visualized using the Amersham ECL detection kit (Cytiva, Marlborough, MA, USA) in a ChemiDoc imaging system (Bio-Rad, Hercules, CA, USA). For determination of size of proteins and testing of specificity of rabbit antisera, 0.25 µg of purified EfaA, AdcA, and AdcAII were added to 12% separating tris-glycine gel and visualized after staining in coomassie blue solution (0.25% (w/v) Coomassie blue R250).

Galleria mellonella infection

To assess *E. faecalis* virulence, the larvae of *G. mellonella* were infected as described previously (Colomer-Winter et al. 2018). Briefly, larvae (groups of 20) were injected with either (i) *E. faecalis* OG1RF alone ($\sim 5 \times 10^5$ CFU), (ii) OG1RF pre-absorbed with rabbit antisera at a dilution of 1:20 for 1 hour at 37°C, (iii) heat-killed OG1RF (30 mins at 100°C), or (iv) vehicle controls (PBS or rabbit antisera). Post-injection, larvae were kept at 37°C and their survival recorded over time.

IP challenge mouse model

The methods for the peritonitis model have been published (Kajfasz et al. 2012), such that only a brief overview that includes minor modifications is described here. To assess colonization burden, female 8-week-old C57BL/6 J mice (Jackson Laboratories, Bar Harbor, ME, USA) were injected IP with $\sim 5 \times 10^8$ CFUs of bacteria from an overnight culture, and euthanized either 48 hours or 96 hours post-injection to determine bacterial burden in spleen, kidneys, and the peritoneal cavity. To assess the significance of passive immunization on recovered bacterial titers, mice received IP injections of 200 µl of either PBS, antisera pre-bleed (pooled from rabbits from each group), or antisera obtained after single or multiple antigen immunization (pooled from 3 rabbits per group), 48 and 24 hours before the bacterial challenge, with another boost 24 hours after infection. To determine efficacy of active immunization on bacterial burden, mice received subcutaneous injections containing 5 µg of antigen on days 1, 21, and 42. Complete Freud's adjuvant (CFA) and incomplete Freud's adjuvant (IFA) (Thermo Scientific, Waltham, MA, USA) was mixed with antigens and injected at a final volume of 100 µl for initial and subsequent immunizations, respectively. PBS was used as the vehicle control. In active immunization studies, bacterial challenge was performed 7 days after the final immunization. Determination of bacterial titers was performed by plating serially diluted aliquots of homogenized tissues on BHI plates. To assess efficacy of active immunization against lethal infection, $\sim 2 \times 10^9$ CFUs of bacteria were injected via IP after completion of the active immunization regimen. Then, mice were monitored for survival over a course of 3 days. For survival experiments, animals were closely assessed for signs of behavior and neurological deteriorations that warrants humane euthanasia using a clinical scoring system approved by the University of Florida (UF) Institutional Animal Care and Use Committee (IACUC). All mouse procedures were previously approved and performed in compliance with the UF IACUC (Protocol: 202 200 000 241).

Statistical analysis

Data obtained from this study were analyzed using GraphPad Prism 9.0 software (GraphPad Software, San Diego, CA, USA). Data from multiple experiments conducted on non-consecutive days were collated and applicable statistical tests were used. Only comparisons of groups in each dataset, that is appropriate in the context of results interpretation and discussion, were analyzed. Unless stated otherwise, only comparisons with significant differences (P-value < 0.05) indicated with their corresponding asterisks will be noted in the figure legends. Comparisons with no significance differences do not have asterisks signs.

Results

Generation of recombinant EfaA, AdcA, and AdcAII poteins and antisera

Recombinant AdcA (protein ID: WP_002367576.1), AdcAII (protein ID: WP_002392710.1), and EfaA (protein ID: WP_002356954.1) were obtained using Vaxcyte's XpressCF+^{TM} platform (Zawada et al. 2011). His-tagged AdcA, AdcAII, and EfaA proteins were purified using affinity chromatography followed by TeV cleavage of the N-terminal His-6 tag. After cleavage, EfaA and AdcA yielded single bands that migrated near their predicted molecular masses, while purified AdcAII showed a band migrating at the predicted size but also signs of degradation (Fig. 1A). After further purification of pooled eluted fractions using a size exclusion column with a MW cutoff of 10 kDa, we performed the biophysical characterization of each purified protein using SEC-MALS that revealed that the MW of EfaA (30.7 kDa), AdcA (32.2 kDa), and AdcAII (54.7 kDa) (Fig. 1B) are in close approximation to the predicted MW of these proteins reported in the BioCyc database (EfaA; 34.7 kDa, AdcA; 35.1 kDa, AdcAII; 57.6 kDa) (Karp et al. 2019). Purified proteins were then used to raise single-antigen and multi-antigen (EfaA + AdcAII or EfaA + AdcA + AdcAII) antisera in rabbits. To verify that single-antigen antisera were specific to *E. faecalis* EfaA, AdcA, and AdcAII, we performed immunoblot analyses with each antisera using total protein lysates from *E. faecalis* OG1RF and respective isogenic deletion strains lacking EfaA (Δ*efa*) (Colomer-Winter et al. 2018) or both AdcA and AdcAII (Δ*adc*Δ*adcAII*) (Lam et al. 2022). With the EfaA antisera, we observed a single band that corresponded to the size of EfaA in the parent strain lane but (as expected) not in the Δ*efa* mutant (Fig. 1C). In addition to reacting to AdcA, the AdcA antisera cross-reacted with AdcAII, but reacted more strongly with AdcA than AdcAII in the parent strain lysate (Fig. 1D). Pairwise alignment indicates that AdcA shares 56% identity with the larger AdcAII (Fig. S1). Similar to the AdcA antisera, AdcAII antisera cross-reacted with purified AdcA but reacted more strongly with AdcAII than AdcA (Fig. 1E). We next performed ELISAs to determine IgG titers of both single- and multi-antigen immunized groups. Antibody titers were compared using sera obtained prior to immunization (pre-bleed) and after completion of the immunization cycle (terminal bleed). Lipoteichoic acid (LTA) from *Staphylococcus aureus* and antisera derived from immunization with alum (adjuvant/vehicle control) were used to verify that binding of antisera to each protein of interest was specific. All antisera displayed baseline IgG titers against *S. aureus* LTA, EfaA, AdcA, and AdcAII that did not significantly increase after immunization with alum (Fig. 1F and G). Immunization with EfaA, AdcA, or AdcAII increased corresponding IgG titers by ∼100-fold and, as expected, AdcA and AdcAII antisera cross-react with AdcA or AdcAII, respectively (Fig. 1F). Of note, immunization with either EfaA + AdcAII or EfaA + AdcA + AdcAII combinations yielded similarly high levels of IgG titers against all three proteins (Fig. 1G).

Antisera derived from multi-antigen immunization contain opsonic antibodies, like their single antigen counterparts

To determine whether multi-antigen (EfaA + AdcAII, and EfA + AdcA + AdcAII) antisera contain more (or at least similar) opsonic antibodies to single (EfaA, AdcA, or AdcAII) antigen antisera, we evaluated the capacity of each antiserum to mediate bacterial killing in an opsonophagocytic assay (OPA). When compared to the corresponding pre-bleed counterparts, antisera of mice immunized with single-antigen EfaA (49%), AdcA (35%), and AdcAII (43%), respectively, had increased opsonic antibodies. Similarly, antisera of mice immunized with 2- (50%) or 3-antigen (41.5%) had increased opsonic antibodies (Fig. 2A). In controls that lack either the complement, neutrophils, or both components resulted in no killing of *E. faecalis* (Fig. S2A). Because sonication of cells (post incubation with 1:10 sera dilution) did not increase CFUs recovered, and further dilution of the trivalent sera exhibited a dose-dependent killing efficacy, we conclude that agglutination of *E. faecalis* cells is not occurring in these concentrations of antisera used (Fig. S2B). To confirm specificity of these results, single antigen antisera were pre-incubated with corresponding protein to block antibody-dependent opsonization. As anticipated, pre-incubation with corresponding antigen significantly reduced (α-EfaA; 80.16%, α-AdcA; 81.5%, α-AdcAII; 68.7%) the opsonic killing capacity of each antiserum in a concentration-dependent manner when compared to the negative control bovine serum albumin (BSA) (Fig. 2B).

Antibodies against EfaA, AdcA, and AdcAII synergize with calprotectin to inhibit *E. faecalis* growth

It is well established that manganese and zinc are primarily sequestered by calprotectin (CP) (Damo et al. 2013, Clark et al. 2016), a member of the S100 protein family produced in large quantities by neutrophils and other immune cells during infection and inflammation (Palmer and Skaar 2016). In previous studies, we showed that growth of the Δ*efa* mutant is strongly inhibited by purified human CP (hCP) but not by a hCP variant that cannot chelate manganese (Colomer-Winter et al. 2018). Furthermore, growth of the Δ*adc*AΔ*adcAII* mutant was severely inhibited by hCP but restored by zinc supplementation in a concentration-dependent manner (Lam et al. 2022). Next, we asked if antibodies against EfaA, AdcA, and AdcAII can potentiate the growth inhibitory effects of hCP by further hindering the ability of EfaA and AdcA/AdcAII to scavenge manganese or zinc from an environment rich in CP. To do so, we compared the ability of *E. faecalis* OG1RF to grow in BHI-CB, a laboratory media that contains ∼10 μM zinc and 0.57 μM manganese (Brunson et al. 2023), or BHI-CB supplemented with either calprotectin (hCP), a mixture of α-EfaA, α-AdcA, α-AdcAII purified antibodies (herein referred as ∞-3Abs), or both hCP and ∞-3Abs. While bacterial growth was considerably slower in media supplemented with hCP, final growth yields were similar to those attained by cultures grown in media without hCP (Fig. 3A). On the other hand, growth in the presence of ∞-3Abs displayed similar exponential growth but final growth yields were slightly lower when compared to media-only control (Fig. 3A). In the next set of experiments, we showed that combination of hCP with the ∞-3Abs mixture slowed growth and significantly reduced final growth yields, while combination of hCP with each single-antigen antibodies alone resulted in modest reductions of final growth yields (Fig. 3B). Next, we assessed the fitness of *E. faecalis* OG1RF in pooled human sera supplemented with either native calprotectin (hCP) or the manganese-deficient CP variant (hCP$^{\Delta Mn}$), ∞-3Abs, or combinations of hCP or hCP$^{\Delta Mn}$ with ∞-3Abs using heat-inactivated ∞-3Abs (HI ∞-3Abs) as negative control. When compared to serum alone, growth in serum supplemented with ∞-3Abs was modestly reduced (∼1.9-fold) but not when compared to serum containing HI-∞-3Abs (Fig. 3C). Addition of either hCP or hCP$^{\Delta Mn}$ alone had a negligible impact on OG1RF viability when compared to serum only. However, the combination of hCP and ∞-3Abs significantly reduced growth yields when compared to serum only (5.25-fold) or serum + ∞-3Abs (2.77-fold) (Fig. 3C). Notably, this synergism was not significant

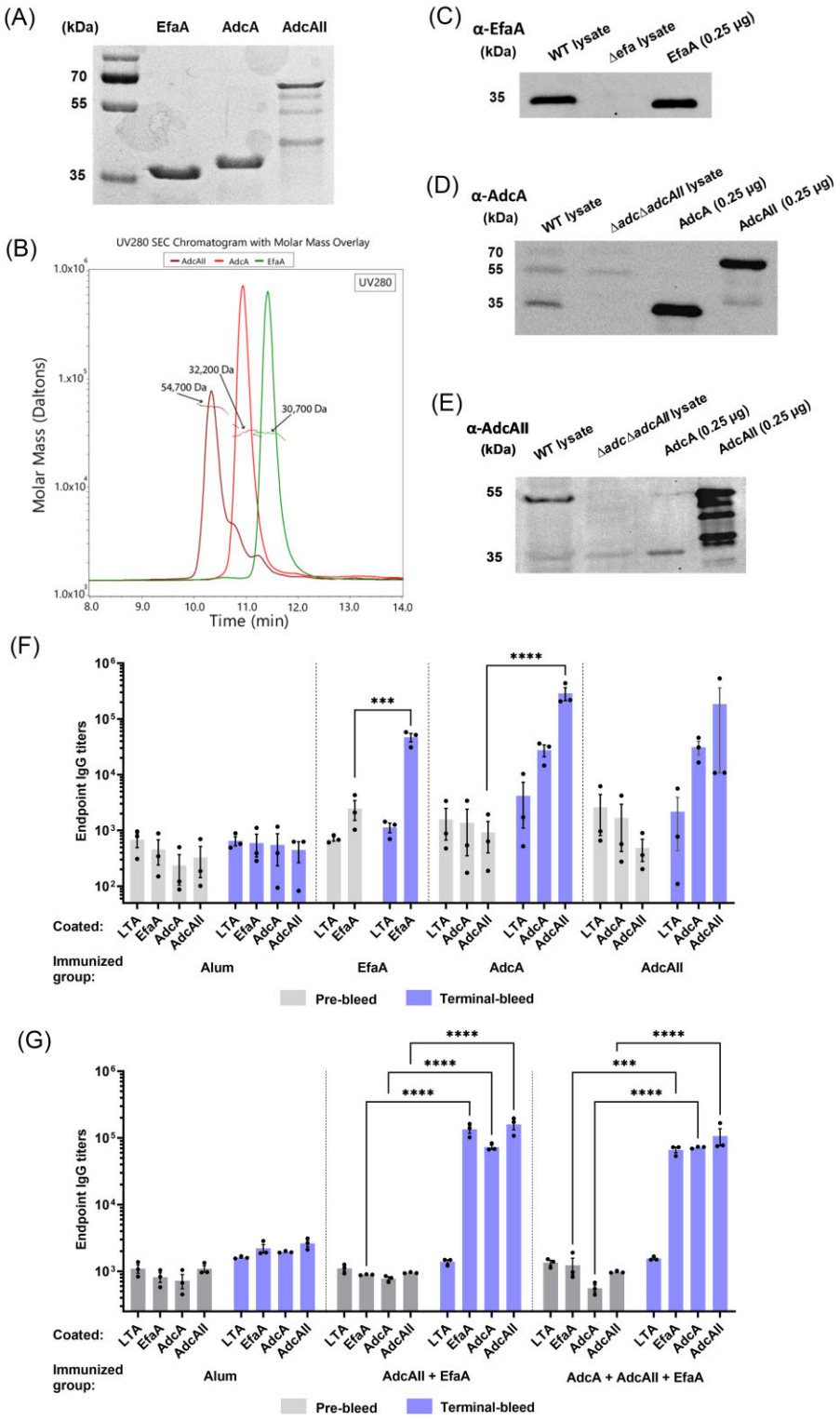

Figure 1. Antisera antibodies against EfaA, AdcA, and AdcAII are highly specific. (A) Coomassie blue-stained protein blot loaded with 2 µg of recombinant EfaA, AdcA, and AdcAII, respectively, and 2 µl of protein ladder. (B) SEC-MALS analysis of weight-averaged masses (Mw) of recombinant proteins in solution by measuring the intensity of scattered light from these samples as it elutes from an SEC column. (C) Immunoblot showing EfaA expression in whole cell lysates of *E. faecalis* WT cells and Δ*efa* cells that has been normalized to 100 µg of total protein, and then compared with 0.25 µg recombinant EfaA. Immunoblot showing (D) AdcA and (E) AdcAII expression in whole cell lysates of *E. faecalis* WT cells and Δ*adc*Δ*adcAII* cells that has been normalized to 100 µg of total protein, and compared with 0.25 µg recombinant AdcA and AdcAII, respectively. The images shown in B–D are representative from three experiments using three biological replicates. (F–G) ELISA endpoint titers showing binding of recombinant EfaA, AdcA, and AdcAII, respectively, to lipoprotein-specific sera/antisera IgG harvested from rabbits immunized with (F) single antigen or (G) combinations of antigens. For E, data points represent average titers of three repeated experiments using rabbit sera ($n = 1$) of each immunization group. For G, data points represent average titers of three repeated experiments using pooled rabbit sera ($n = 3$) of each immunization group. For F and G, statistical analysis was performed using two-way ANOVA with Turkey's multiple comparison test. *** $P \leq 0.001$, **** $P \leq 0.0001$. Error bars represent the standard error of margin (SEM).

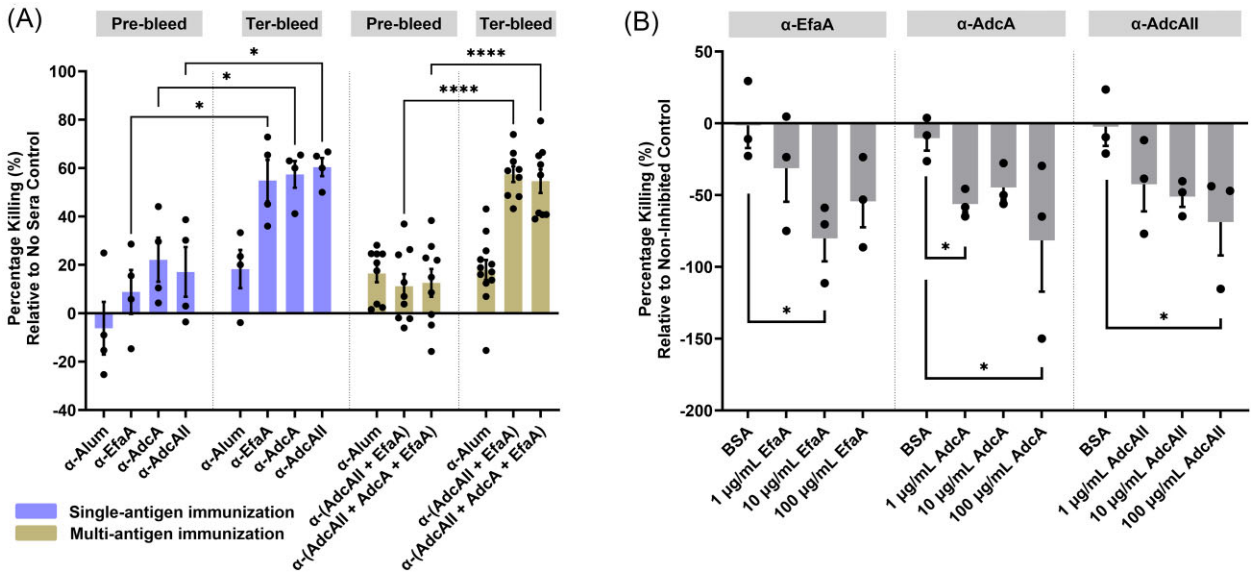

Figure 2. Lipoprotein-specific antisera, both singly or in combination, enhance neutrophil-mediated opsonization. (A) Percentage of *E. faecalis* OG1RF cells subjected to opsonic killing via antibody-mediated neutrophil opsonization using rabbit antisera obtained from single-antigen and multi-antigen immunization, respectively. Pre-immunization rabbit sera, termed pre-bleed, is used as sera control. Each data point represents average of 3 biological replicates of *E. faecalis* OG1RF tested with one rabbit antisera (rabbit sera; $n = 1$ for single-antigen sera groups and $n = 3$ for multi-antigen sera groups) in a single experiment. For all sera groups, experiments have been repeated at least on three non-consecutive days. Statistical analysis was performed using *t* test with Welch's correction. To inhibit antibody-mediated neutrophil opsonization of *E. faecalis*, (B) EfaA, AdcA, and AdcAII antisera obtained from single-antigen immunization, respectively, were pre-incubated with increasing concentrations of their corresponding antigen of interest and a non-inhibitory protein control, bovine serum albumin (BSA; 100 μg ml^{-1}) prior to bacterial exposure. Statistical analysis was performed using Kruskal–Wallis test. Data point represents average from at least 2 repeated, non-consecutive experiments using 3 biological replicates of *E. faecalis*. Error bars represent the standard error of margin (SEM). For A–B, pooled neutrophils in each experiment were harvested from 7 to 8 de-identified human donors. * $P \leq 0.05$, *** $P \leq 0.001$, **** $P \leq 0.0001$.

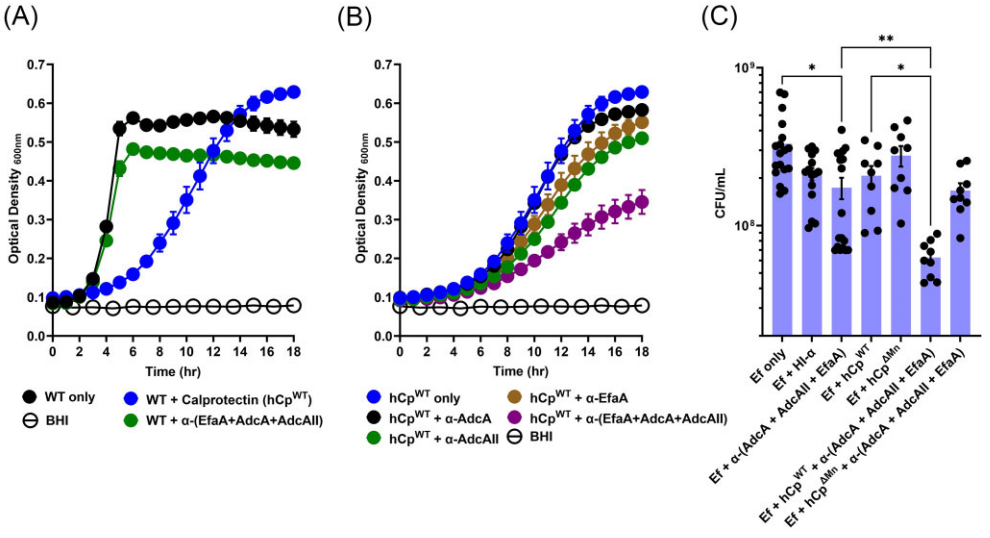

Figure 3. Lipoprotein-specific antibodies act in concerted effort with calprotectin to restrict *E. faecalis* ability to grow and acquire metals. Growth of *E. faecalis* OG1RF (WT) in BHI-CB media that has been supplemented with (A) calprotectin (150 μg ml^{-1}) and affinity purified antibodies cocktail (α-EfaA, α-AdcA, and α-AdcAII) (25 μg ml^{-1}), respectively, or (B) combination of calprotectin (150 μg ml^{-1}) with one or more of the antibodies (α-EfaA, α-AdcA, and α-AdcAII) (25 μg ml^{-1}). Data points represent the average of nine biological replicates. Statistical analysis was performed using simple linear regression of exponential growth phase, and slope of each test condition was compared to the control (A; WT only or B; CP^{WT} only), respectively. (C) CFU of *E. faecalis* OG1RF recovered *ex vivo* from pooled human serum supplemented with (A) calprotectin (WT or ΔMn) (150 μg ml^{-1}), and antibodies cocktail (α-EfaA, α-AdcA, and α-AdcAII) (25 μg ml^{-1}), respectively, or in combination after incubation for 24 hours. Heat-inactivated antibodies (α-EfaA, α-AdcA, and α-AdcAII) (25 μg ml^{-1}) (HI-α) were prepared by heating at 65 degrees for 1 hour, and used as control. Data points represent nine to twelve biological replicates after running ROUT standard 1% outlier test. Data analysis was performed using Brown-Forsythe ANOVA test with Dunnett's T3 multiple comparison test. Error bars represent the standard error of margin (SEM). * $P \leq 0.05$, ** $P \leq 0.01$.

when ∞-3Abs was combined with hCP$^{\Delta Mn}$. While mechanisms remain to be determined, these results strongly suggest that these EfaA-, AdcA-, and AdcAII-specific antibodies restrict the growth of *E. faecalis* under metal-depleted conditions *in vitro*.

Trivalent immunization mediates *E. faecalis* clearance and enhances host survival rates in a mouse model of peritonitis

Next, we used two *in vivo* models to evaluate whether passive transfer of multi-antigen antisera can provide stronger protection against *E. faecalis* infection, when compared to their single-antigen counterparts. In the *G. mellonella* model, administration of either 2- (EfaA+AdcAII) or 3-antigen (EfaA+AdcA+AdcAII) antisera, but not single antigen antisera, significantly increased larvae survival (~35%) from a lethal infective dose of *E. faecalis* OG1RF (Fig. 4A and B, control injections with antisera only, PBS, or heat-inactivated *E. faecalis* are shown in Fig. S2). The data obtained from the *G. mellonella* model provided compelling reasons for us to further investigate the protective properties of these antisera in a systemic infection model. Using an IP challenge mouse model that spreads systemically within 24 hours, passive immunization with single antigen antisera reduced bacterial burden at the site of infection (peritoneal cavity) and systemically (spleen and kidney) by ~0.5 to 1-log, albeit the protection conferred by AdcA antisera in the spleen, and AdcAII antisera in the peritoneal cavity was not significant when compared to alum control antisera (Fig. 4C). While no significant differences were seen between bacterial recovery (at the different sites) of the controls (alum, pooled pre-bleed sera, PBS), there was larger variability in CFUs recovered from mice passively immunized with EfaA, AdcA, and AdcAII from spleen and kidney. In contrast, both 2- and 3-antigen antisera enhanced protection against infection (0.5 to 1-log), and appear to have more consistent recovery of bacterial burden throughout all sites, despite alum control antisera in this experiment providing significant (and unexpected) protection when compared to the PBS control (Fig. 4D).

Next, we explored the protective effects of active immunization with EfaA, AdcA, and AdcAII using the IP challenge mouse model. Consistent with the results of passive immunization, we observed that animals immunized with the 3-antigen combination were more rapidly cleared (1-log reduction) from infection in the spleen and peritoneal cavity compared to the adjuvant-only control group 48- and 96-hours post-infection, with the titers observed in the kidneys at 48 hours being the only comparison failing to reach statistical significance (Fig. 5A–C). Finally, active immunization with the 3-antigen combination, but not the single antigen counterparts, significantly improved survival rates of mice infected with a lethal of *E. faecalis* OG1RF dose by ~30% (Fig. 5D).

EfaA, AdcA, and AdcAII as scaffolds for the development of a broadly protective multivalent enterococcal vaccine

Given the high conservation of *E. faecalis* EfaA (Fig. S3), AdcA (Fig. S4A), and AdcAII (Fig. S4B) among clinical isolates of *E. faecalis* and their relative conservation in clinical *E. faecium* strains, we further investigated whether immunization with the 3-antigen cocktail could protect against infection by clinical *E. faecalis* and *E. faecium* strains. Initially, we examined the opsonic killing capacity of the 3-antigen (EfaA + AdcA + AdcAII) antisera against a panel of *E. faecalis* and *E. faecium* clinical isolates (both MDR and non-MDR). Our findings revealed that the 3-antigen antisera enhanced neutrophil-mediated opsonophagocytic killing of both *E. faecalis* and *E. faecium* isolates to levels comparable to those obtained for *E. faecalis* OG1RF (Fig. 6A and B). Subsequently, we investigated the protective effects of active immunization on mice infected with one *E. faecalis* and *E. faecium* clinical isolate, respectively. Our results demonstrated that immunization with the 3-antigen cocktail enhanced systemic clearance of both *E. faecalis* TX0104 and *E. faecium* ERV99 in spleens (0.5-log, 0.5-log) and kidneys (1-log, 0.5-log), although it did not reduce bacterial burden in the peritoneal cavity (Fig. 6C–E). While these findings are indeed encouraging, we are optimistic that this trivalent antigen combination could potentially serve as the scaffold to build a multivalent, broadly protective enterococcal vaccine formulation in the future.

Discusssion

Despite the undeniable efficacy of vaccination in preventing infectious diseases and the persistent threat posed by enterococcal infections, a recent review examining vaccines targeting MDR pathogens revealed that there are currently no vaccines in either the pre-clinical or clinical development stages targeting either *E. faecalis* or *E. faecium* (Frost et al. 2023). Nevertheless, studies conducted by a selected number of laboratories have identified several protein and polysaccharide targets that have elicited opsonic antibodies. In some cases, these targets have demonstrated the ability to confer protection against *E. faecalis* infections. (Singh et al. 2010, Theilacker et al. 2011, Flores-Mireles et al. 2014, Kazemian et al. 2019, Wagner et al. 2023). While *E. faecium* accounts for a smaller fraction of human enterococcal infections, treatment of *E. faecium* infections tends to be more challenging due to the considerable higher prevalence of *E. faecium* MDR strains compared to *E. faecalis* (Moghimbeigi et al. 2018, Boccella et al. 2021, Dadashi et al. 2021). As a result, there has also been a recent interest in the development of vaccines against MDR *E. faecium* (Nallapareddy et al. 2008, Kropec et al. 2011, Kodali et al. 2015, Wagner et al. 2023). But there are also promising studies that identified common antigens that can be used to develop a broad-spectrum multivalent vaccine capable of effectively targeting both *E. faecalis* and *E. faecium* (Laverde et al. 2014, Romero-Saavedra et al. 2014, Romero-Saavedra et al. 2019).

Among prior investigations, Huebner and colleagues showed that antibodies raised against *E. faecium* E155 AdcA$_{fm}$ (73% and 57% similarity with *E. faecalis* OG1RF AdcA and AdcAII, respectively) and PsaA$_{fm}$ (63% similarity with *E. faecalis* OG1RF EfaA) have opsonic properties and provide protection against *E. faecium* systemic dissemination in a mouse model (Romero-Saavedra et al. 2015). Because metal-binding proteins are conserved among Gram-positive bacteria, are critical for bacterial fitness, and have been shown to trigger robust immune responses, there have been attempts to exploit them as vaccine antigen. One example is the EfaA/PsaA$_{fm}$ homologue from *S. pneumoniae*, known as PsaA, which was shown to protect against pneumococcal nasal carriage in a mouse model (Briles et al. 2000), and has been included in multivalent protein-based vaccine formulations (Entwisle et al. 2017, Voß et al. 2018, Chan et al. 2019, Bahadori et al. 2024). Other examples are co-immunization with *S. pneumococcus* PiuA and PiA (both iron-binding lipoproteins) and *S. aureus* MntC (manganese-binding) that protected mice from subsequent infection by the corresponding pathogen (Jomaa et al. 2006, Anderson et al. 2012). An important aspect to consider when developing an enterococcal vaccine is whether it will provide broad protection across different strain lineages, particularly regarding specific targeting of virulence factors. Progress in vaccine development is further com-

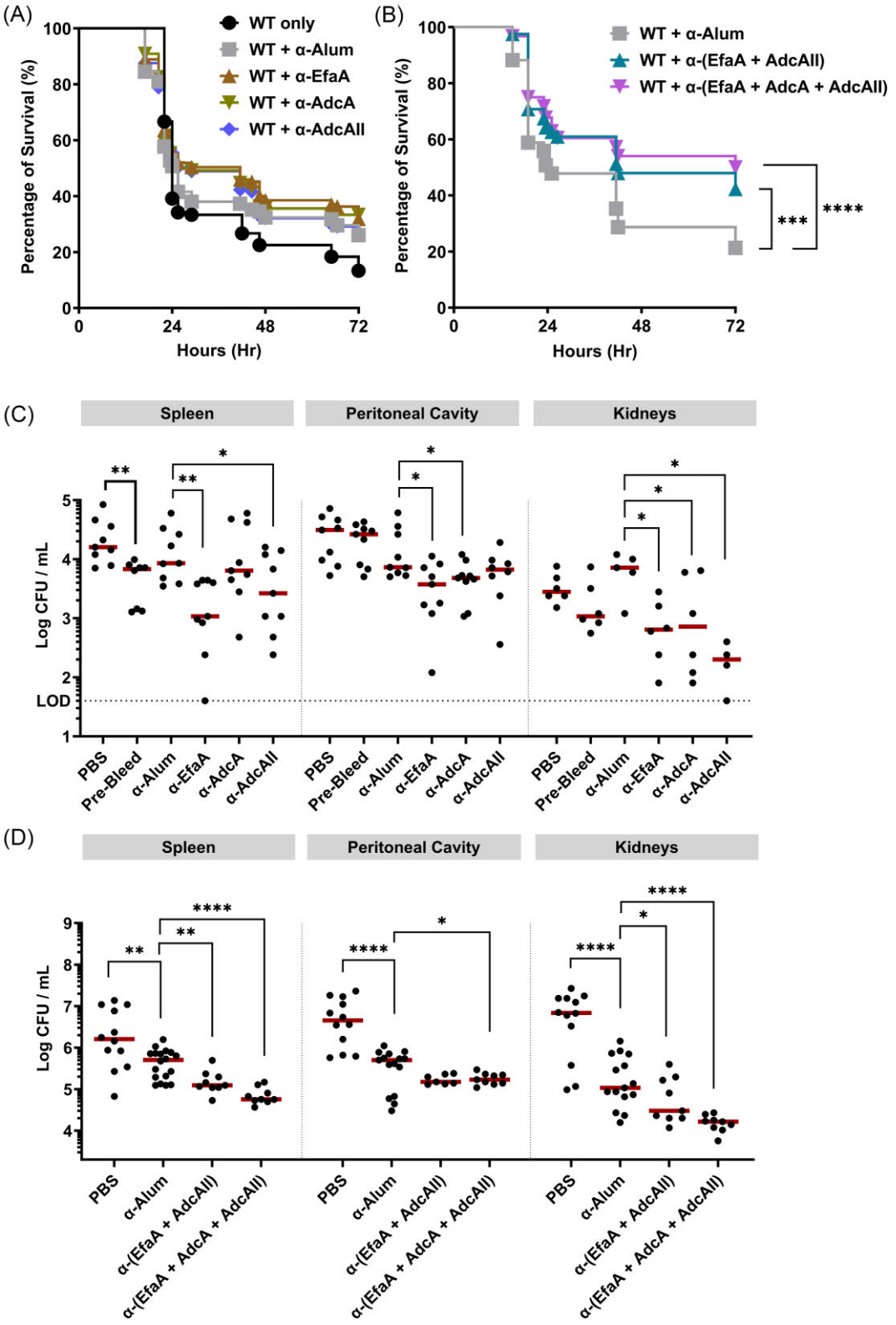

Figure 4. Passive transferred antibodies confer protection during *E. faecalis* infection. Percentage survival of *G. mellonella* larvae 96 hours post-infection with *E. faecalis* WT alone, or pre-incubated together with (A) single-antigen and (B) multi-antigen antisera at a ratio of 1:20. Each curve represents a group of 20 larvae injected with ~1×10^5 CFU of *E. faecalis* WT. Data points represent average of six biological replicates. Statistical analysis was performed using Log-rank (Mantel–Cox) test. *** $P \leq 0.001$, **** $P \leq 0.0001$. For passive immunization studies, total CFU was recovered after 48 hours post-infection from spleen, peritoneal cavity, and kidneys of mice immunized with (C) single-antigen antisera and (D) multi-antigen antisera, respectively. PBS (mock infected) and pre-bleed (sera control) are used as negative controls. Data points represent groups of mice immunized with single-antigen ($n = 9$) and multi-antigen ($n = 12$), respectively, using two biological replicates of *E. faecalis* OG1RF. After running ROUT standard 1% outlier test, statistical analysis was performed using Mann–Whitney test. * $P \leq 0.05$, ** $P \leq 0.01$, **** $P \leq 0.0001$. The dashed line represents the limit of detection (LOD = 40 CFUs).

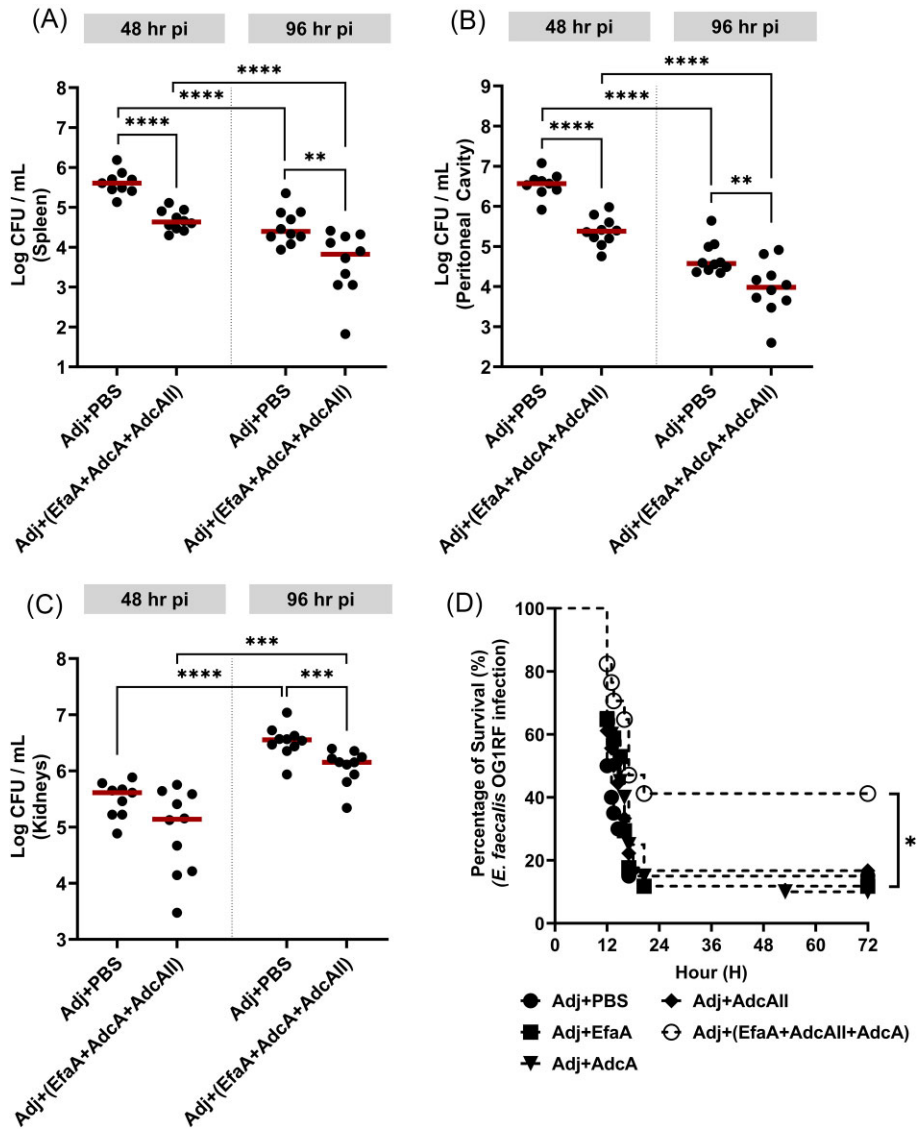

Figure 5. Active immunity enhances systemic bacterial clearance and confers protection from lethal doses of *E. faecalis* infection. For active immunization studies, total CFU was recovered after 48 and 96 hours post-infection, respectively, from (A) spleen, (B) peritoneal cavity, and (C) kidneys of mice immunized with antigen cocktail (EfaA + AdcA + AdcAII) suspended in Freud's adjuvant. PBS suspended in Freud's adjuvant is used as immunization control. Data points represent groups of 10 infected mice using two biological replicates of *E. faecalis* OG1RF. After running ROUT standard 1% outlier test, statistical analysis was performed using Mann–Whitney test. ** $P \leq 0.01$, *** $P \leq 0.001$, **** $P \leq 0.0001$. (D) Percentage survival of mice immunized with either antigen cocktail (EfaA + AdcA + AdcAII) or their single-antigen counterparts 72 hours post-infection with lethal dose of *E. faecalis* OG1RF. Mice immunized with PBS suspended in Freud's adjuvant are used as immunization control. Each curve represents a group of 20 mice. Data points represent average of 2 biological replicates. Statistical analysis was performed using Log-rank (Mantel–Cox) test. * $P \leq 0.05$.

plicated by strain heterogeneity, which includes the existence of encapsulated strains of *E. faecalis* and *E. faecium*, as well as the lack of a consensus as to which factors (if any) separate pathogenic enterococci from non-pathogenic enterococci. Previous studies have used capsular enterococcal polysaccharides alone or conjugated with enterococcal-specific proteins, or other protein carriers, as an attempt to increase protection coverage with somewhat encouraging results (Kodali et al. 2015, Romero-Saavedra et al. 2019). Here, we showed that antibodies against EfaA, AdcA, and AdcAII enhance opsonophagocytic killing against both non-capsule producer (OG1RF, serotype B) and capsule-producer (MMH594, serotype C) *E. faecalis* strains, suggesting that these antigens are not hidden from immune recognition by capsular cell wall components.

The present investigation validates and expands the findings of Romero-Saavedra and colleagues as rabbit antisera raised against EfaA, AdcA, or AdcAII facilitated neutrophil-mediated opsonization when tested against clinical strains of *E. faecalis* and *E. faecium*, and conferred robust to moderate protection against *E. faecalis* systemic dissemination when administered prior to an IP challenge. In addition, we showed that EfaA, AdcA, and AdcAII antibodies have growth-inhibitory properties, and that antisera raised against two (EfaA and AdcAII) or all three antigens confers more robust protection than single antigen antisera. Finally, the results from our study demonstrate that active immunization with the 3-antigen cocktail provides protection against both non-lethal and lethal intraperitoneal challenges, using two distinct strains of *E. faecalis* and one strain of *E. faecium*. These findings present com-

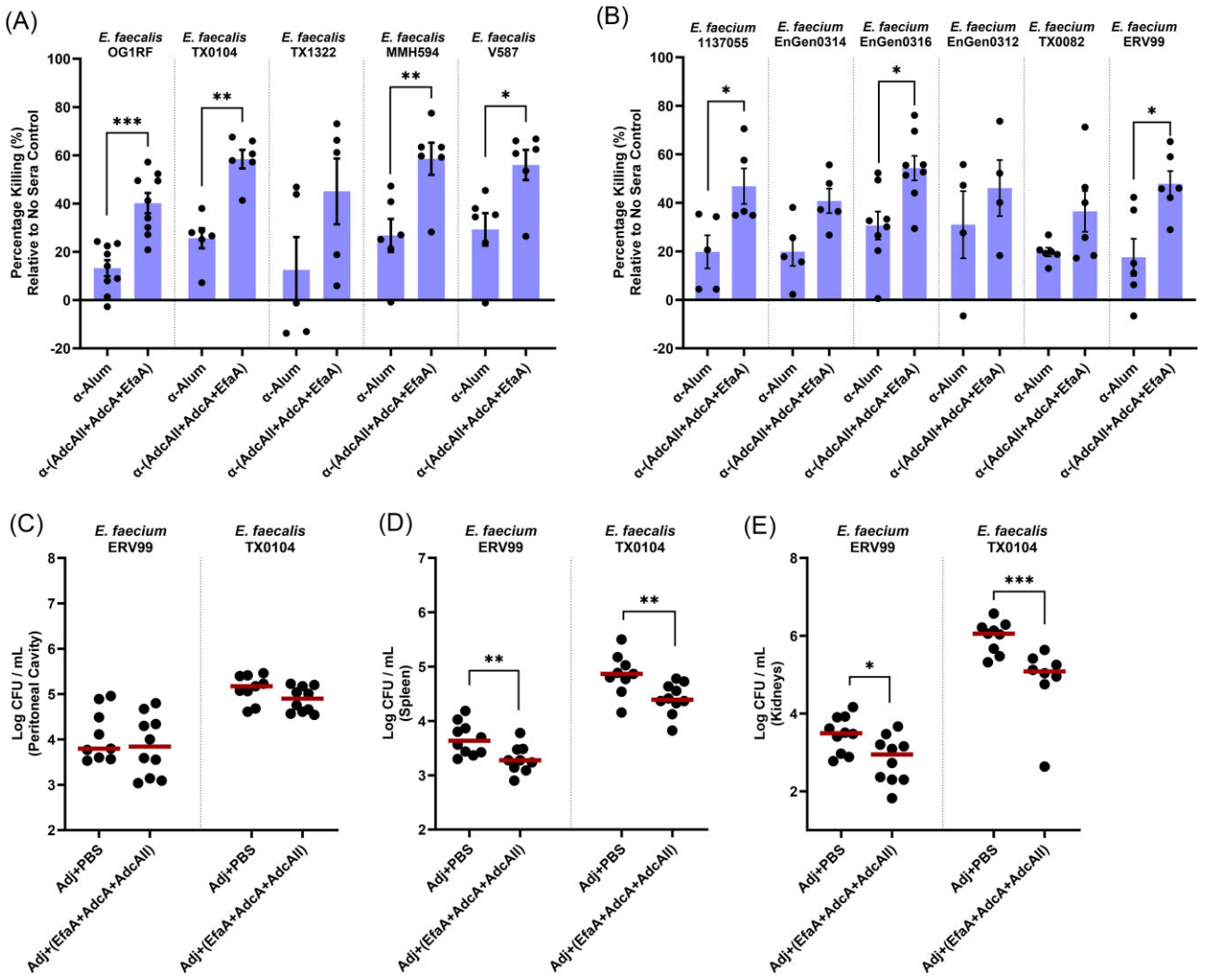

Figure 6. Targeting metal-binding lipoproteins confer broad protection against *E. faecalis* and *E. faecium* clinical strains. Using *E. faecalis* OG1RF as a reference strain, percentage of opsonic killing via antibody-mediated neutrophil opsonization using multi-antigen antisera (EfaA + AdcA + AdcAII) was compared against a list of (A) *E. faecalis* and (B) *E. faecium* clinical strains. Alum antisera is used as sera control. Each data point represents the average of 3 biological replicates of *E. faecalis* OG1RF tested in a single experiment. For all sera groups, experiments have been repeated at least on four non-consecutive days. Error bars represent the standard error of margin (SEM). For A–B, pooled neutrophils in each experiment were harvested from 7 to 8 de-identified human donors. Statistical analysis was performed using unpaired *t*-test with Welch's correction. * $P \leq 0.05$, ** $P \leq 0.01$, *** $P \leq 0.001$. For active immunization studies, total CFUs were recovered from (C) peritoneal cavity, (D) spleen, and (E) kidneys after 48 hours post-infection with clinical isolates *E. faecium* ERV99 and *E. faecalis* TX0104, respectively. Data points represent groups of 10 infected mice, using two biological replicates. After running ROUT standard 1% outlier test, statistical analysis was performed using Mann–Whitney test. *$P \leq 0.05$, **$P \leq 0.01$, ***$P \leq 0.001$.

pelling evidence of the promise of these metal-binding proteins as vaccine immunogens.

It is widely acknowledged that multivalent vaccine formulations elicit superior and broader immune protection compared to monovalent formulations. Therefore, our future efforts will focus on leveraging the high-throughput capacity of XpressCF™ technology to explore additional enterococcal proteins that can be combined with EfaA and AdcAII to generate a multivalent formulation that can more efficiently (and specifically) target multiple serotypes of *E. faecalis* and *E. faecium*. Along these lines, we recently identified two novel metal-binding lipoproteins, named EmtC and FitD, which were shown to work in concerted effort with EfaA and two other transporters to mediate iron uptake in *E. faecalis* (Brunson et al. 2023). Notably, EmtC and FitD are ubiquitous to *E. faecalis* and, to the best of our knowledge, restricted to the Enterococcaceae family with the closest non-enterococcal homologues (found in few Streptococci and Bacilli) sharing ~60%–65% similarity with FitD. Building upon the results obtained here, the incorporation of EmtC, FitD, or both to a backbone formulation containing EfaA and at least AdcAII holds the potential to augment vaccine coverage, efficacy, and specificity. This enhancement could be achieved by further disrupting bacterial trace metal homeostasis while simultaneously boosting opsonophagocytic activity and fostering long-term immunological memory. In addition, immunogenic surface-associated virulence factors such as Ace and EbpA can be added to the multivalent vaccine formulation to specifically tackle host colonization factors previously shown to play important roles in *E. faecalis* virulence in CAUTI and endocarditis (Flores-Mireles et al. 2014, Singh et al. 2018). In conclusion, our study has demonstrated the feasibility of EfaA, AdcA, and AdcAII as promising candidates for the development of a broadly protective multivalent vaccine against enterococcal infections. While additional research is necessary to explore their potential, we have no doubt that a broad-spectrum enterococcal vaccine will

be beneficial for patients, their caregivers, and healthcare professionals, who are at elevated risk of developing enterococcal infections.

Acknowledgments

We thank Phil Fernstein for helpful discussions.

Supplementary data

Supplementary data is available at *FEMSMC Journal* online.

Conflict of interest: J.F. is co-founder and employed at Vaxcyte, Inc. A.S. and A.B. are employed at Vaxcyte.

Funding

This study was supported by Vaxcyte, Inc. (ID: AGR00021384) and NIH-NIAID R21 (AI137446) awarded to J.L., and American Heart Association (AHA) postdoctoral fellowship (AWD907586) awarded to L.N.L.

Data availability

The authors confirm that the data supporting the findings of this study are available within the article and/or its supplementary materials.

References

Alghamdi F, Shakir M. The influence of *Enterococcus faecalis* as a dental root canal pathogen on endodontic treatment: a systematic review. *Cureus* 2020;**12**:e7257.

Amat-Santos IJ, Ribeiro HB, Urena M *et al.* Prosthetic valve endocarditis after transcatheter valve replacement: a systematic review. *JACC Cardiovasc Interv* 2015;**8**:334–46.

Anderson AS, Scully IL, Timofeyeva Y *et al.* *Staphylococcus aureus* manganese transport protein C is a highly conserved cell surface protein that elicits protective immunity against *S. aureus* and *Staphylococcus epidermidis*. *J Infect Dis* 2012;**205**:1688–96.

Arias CA, Murray BE. The rise of the *Enterococcus*: beyond vancomycin resistance. *Nat Rev Microbiol* 2012;**10**:266–78.

Bahadori Z, Shafaghi M, Sabzevari J *et al.* Design, development, and assessment of a novel multi-peptide vaccine targeting PspC, PsaA, and PhtD proteins of *Streptococcus pneumoniae*. *Int J Biol Macromol* 2024;**258**:128924.

Boccella M, Santella B, Pagliano P *et al.* Prevalence and antimicrobial resistance of *Enterococcus* species: a retrospective cohort study in Italy. *Antibiotics (Basel)* 2021;**10**:1552.

Bowler PG, Duerden BI, Armstrong DG. Wound microbiology and associated approaches to wound management. *Clin Microbiol Rev* 2001;**14**:244–69.

Briles DE, Ades E, Paton JC *et al.* Intranasal immunization of mice with a mixture of the pneumococcal proteins PsaA and PspA is highly protective against nasopharyngeal carriage of *Streptococcus pneumoniae*. *Infect Immun* 2000;**68**:796–800.

Brunson DN, Colomer-Winter C, Lam LN *et al.* Identification of multiple iron uptake mechanisms in *Enterococcus faecalis* and their relationship to virulence. *Infect Immun* 2023;**91**:e0049622.

Chan WY, Entwisle C, Ercoli G *et al.* A novel, multiple-antigen pneumococcal vaccine protects against lethal *Streptococcus pneumoniae* challenge. *Infect Immun* 2019;**87**:e00846–18.

Chanderraj R, Brown CA, Hinkle K *et al.* Gut microbiota predict *Enterococcus* expansion but not vancomycin-resistant vancomycin-resistant *Enterococcus* acquisition. *mSphere* 2020;**5**:e00537–20.

Clark HL, Jhingran A, Sun Y *et al.* Zinc and manganese chelation by neutrophil S100A8/A9 (calprotectin) limits extracellular *Aspergillus fumigatus* hyphal growth and corneal infection. *J Immunol* 2016;**196**:336–44.

Colomer-Winter C, Flores-Mireles AL, Baker SP *et al.* Manganese acquisition is essential for virulence of *Enterococcus faecalis*. *PLoS Pathog* 2018;**14**:e1007102.

Dadashi M, Sharifian P, Bostanshirin N *et al.* The global prevalence of Daptomycin, Tigecycline, and Linezolid-resistant *Enterococcus faecalis* and *Enterococcus faecium* strains from human clinical samples: a systematic review and meta-analysis. *Front Med (Lausanne)* 2021;**8**:720647.

Damo SM, Kehl-Fie TE, Sugitani N *et al.* Molecular basis for manganese sequestration by calprotectin and roles in the innate immune response to invading bacterial pathogens. *Proc Natl Acad Sci USA* 2013;**110**:3841–6.

Dowd SE, Sun Y, Secor PR *et al.* Survey of bacterial diversity in chronic wounds using pyrosequencing, DGGE, and full ribosome shotgun sequencing. *BMC Microbiol* 2008;**8**:43.

Entwisle C, Hill S, Pang Y *et al.* Safety and immunogenicity of a novel multiple antigen pneumococcal vaccine in adults: a Phase 1 randomised clinical trial. *Vaccine* 2017;**35**:7181–6.

Farsi S, Salama I, Escalante-Alderete E *et al.* Multidrug-resistant enterococcal infection in surgical patients, what surgeons need to know. *Microorganisms* 2023;**11**:238.

Fiore E, Van Tyne D, Gilmore MS. Pathogenicity of enterococci. *Microbiol Spectr* 2019;**7**:10. https:// doi.org/10.1128/microbiolspec.GPP1123-0053-2018.

Flores-Mireles AL, Pinkner JS, Caparon MG *et al.* EbpA vaccine antibodies block binding of *Enterococcus faecalis* to fibrinogen to prevent catheter-associated bladder infection in mice. *Sci Transl Med* 2014;**6**:254ra127.

Flores-Mireles AL, Walker JN, Caparon M *et al.* Urinary tract infections: epidemiology, mechanisms of infection and treatment options. *Nat Rev Microbiol* 2015;**13**:269–84.

Forthal DN. Functions of antibodies. *Microbiol Spectr* 2014;**2**:Aid–0019-2014.

Frost I, Sati H, Garcia-Vello P *et al.* The role of bacterial vaccines in the fight against antimicrobial resistance: an analysis of the preclinical and clinical development pipeline. *Lancet Microbe* 2023;**4**:e113–25.

Gaca AO, Lemos JA. Adaptation to adversity: the intermingling of stress tolerance and pathogenesis in enterococci. *Microbiol Mol Biol Rev* 2019;**83**:e00008–00019.

García-Solache M, Rice LB. The *Enterococcus*: a model of adaptability to its environment. *Clin Microbiol Rev* 2019;**32**:e00058–18. https://doi.org/10.1128/cmr.00058-00018.

Gjødsbøl K, Christensen JJ, Karlsmark T *et al.* Multiple bacterial species reside in chronic wounds: a longitudinal study. *Int Wound J* 2006;**3**:225–31.

Hajj Hussein I, Chams N, Chams S *et al.* Vaccines through centuries: major cornerstones of global health. *Front Public Health* 2015;**3**:269.

Hornuss D, Göpel S, Walker SV *et al.* Epidemiological trends and susceptibility patterns of bloodstream infections caused by *Enterococcus* spp. in six German university hospitals: a prospectively evaluated multicentre cohort study from 2016 to 2020 of the R-Net study group. *Infection* 2024. https://link.springer.com/article/10.1007/s15010-024-02249-2#article-info.

Iskandar K, Murugaiyan J, Hammoudi Halat D *et al.* Antibiotic discovery and resistance: the chase and the race. *Antibiotics (Basel)* 2022;**11**:182.

Jansen KU, Gruber WC, Simon R *et al.* The impact of human vaccines on bacterial antimicrobial resistance. A review. *Environ Chem Lett* 2021;**19**:4031–62.

Jomaa M, Terry S, Hale C *et al.* Immunization with the iron uptake ABC transporter proteins PiaA and PiuA prevents respiratory infection with *Streptococcus pneumoniae*. *Vaccine* 2006;**24**:5133–9.

Joyce E, Phull SS, Lorimer JP *et al.* The development and evaluation of ultrasound for the treatment of bacterial suspensions. A study of frequency, power and sonication time on cultured *Bacillus* species. *Ultrason Sonochem* 2003;**10**:315–8.

Kajfasz JK, Mendoza JE, Gaca AO *et al.* The Spx regulator modulates stress responses and virulence in *Enterococcus faecalis*. *Infect Immun* 2012;**80**:2265–75.

Kalfopoulou E, Huebner J. Advances and prospects in vaccine development against enterococci. *Cells* 2020;**9**:2397.

Karp PD, Billington R, Caspi R *et al.* The BioCyc collection of microbial genomes and metabolic pathways. *Briefings Bioinf* 2019;**20**:1085–93.

Kazemian H, Pourmand MR, Siadat SD *et al.* Molecular cloning and immunogenicity evaluation of PpiC, GelE, and VS87_01105 proteins of *Enterococcus faecalis* as vaccine candidates. *Iran Biomed J* 2019;**23**:344–53.

Knapp KG, Goerke AR, Swartz JR. Cell-free synthesis of proteins that require disulfide bonds using glucose as an energy source. *Biotechnol Bioeng* 2007;**97**:901–8.

Kodali S, Vinogradov E, Lin F *et al.* A vaccine approach for the prevention of infections by multidrug-resistant *Enterococcus faecium*. *J Biol Chem* 2015;**290**:19512–26.

Kremserova S, Nauseef WM. Isolation of human neutrophils from venous blood. *Methods Mol Biol* 2020;**2087**:33–42.

Kristich CJ, Rice LB, Arias CA. Enterococcal infection—treatment and antibiotic resistance. Gilmore MS, Clewell DB, Ike Y *et al.* (eds), *Enterococci: From Commensals to Leading Causes of Drug Resistant Infection*. Boston: Massachusetts Eye and Ear Infirmary, 2014.

Kropec A, Sava IG, Vonend C *et al.* Identification of SagA as a novel vaccine target for the prevention of *Enterococcus faecium* infections. 2011;**157**:3429–34.

Lam LN, Brunson DN, Molina JJ *et al.* The AdcACB/AdcAII system is essential for zinc homeostasis and an important contributor of *Enterococcus faecalis* virulence. *Virulence* 2022;**13**:592–608.

Laverde D, Wobser D, Romero-Saavedra F *et al.* Synthetic teichoic acid conjugate vaccine against nosocomial Gram-positive bacteria. *PLoS One* 2014;**9**:e110953.

Mendes RE, Castanheira M, Farrell DJ *et al.* Longitudinal (2001-14) analysis of enterococci and VRE causing invasive infections in European and US hospitals, including a contemporary (2010-13) analysis of oritavancin in vitro potency. *J Antimicrob Chemother* 2016;**71**:3453–8.

Mendes RE, Sader HS, Castanheira M *et al.* Distribution of main Gram-positive pathogens causing bloodstream infections in United States and European hospitals during the SENTRY Antimicrobial Surveillance Program (2010-2016): concomitant analysis of oritavancin in vitro activity. *J Chemother* 2018;**30**:280–9.

Moghimbeigi A, Moghimbeygi M, Dousti M *et al.* Prevalence of vancomycin resistance among isolates of enterococci in Iran: a systematic review and meta-analysis. *Adolesc Health Med Ther* 2018;**9**:177–88.

Murdoch CC, Skaar EP. Nutritional immunity: the battle for nutrient metals at the host–pathogen interface. *Nat Rev Microbiol* 2022;**20**:657–70.

Nallapareddy SR, Singh KV, Murray BE. Contribution of the collagen adhesin Acm to pathogenesis of *Enterococcus faecium* in experimental endocarditis. *Infect Immun* 2008;**76**:4120–8.

Nielsen HV, Flores-Mireles AL, Kau AL *et al.* Pilin and sortase residues critical for endocarditis- and biofilm-associated pilus biogenesis in *Enterococcus faecalis*. *J Bacteriol* 2013;**195**:4484.

Palmer LD, Skaar EP. Transition metals and virulence in bacteria. *Annu Rev Genet* 2016;**50**:67–91.

Romero-Saavedra F, Laverde D, Budin-Verneuil A *et al.* Characterization of two metal binding lipoproteins as vaccine candidates for enterococcal infections. *PLoS One* 2015;**10**:e0136625.

Romero-Saavedra F, Laverde D, Kalfopoulou E *et al.* Conjugation of different immunogenic enterococcal vaccine target antigens leads to extended strain coverage. *J Infect Dis* 2019;**220**:1589–98.

Romero-Saavedra F, Laverde D, Wobser D *et al.* Identification of peptidoglycan-associated proteins as vaccine candidates for enterococcal infections. *PLoS One* 2014;**9**:e111880.

Saleh A, Qamar S, Tekin A *et al.* Vaccine development throughout history. *Cureus* 2021;**13**:e16635.

Singh KV, Nallapareddy SR, Sillanpää J *et al.* Importance of the collagen adhesin ace in pathogenesis and protection against *Enterococcus faecalis* experimental endocarditis. *PLoS Pathog* 2010;**6**:e1000716.

Singh KV, Pinkston KL, Gao P *et al.* Anti-ace monoclonal antibody reduces *Enterococcus faecalis* aortic valve infection in a rat infective endocarditis model. *Pathog Dis* 2018;**76**:fty084.

Theilacker C, Kaczyński Z, Kropec A *et al.* Serodiversity of opsonic antibodies against *Enterococcus faecalis*—glycans of the cell wall revisited. *PLoS One* 2011;**6**:e17839.

Ubeda C, Taur Y, Jenq RR *et al.* Vancomycin-resistant *Enterococcus* domination of intestinal microbiota is enabled by antibiotic treatment in mice and precedes bloodstream invasion in humans. *J Clin Invest* 2010;**120**:4332–41.

Voß F, Kohler TP, Meyer T *et al.* Intranasal vaccination with lipoproteins confers protection against pneumococcal colonisation. *Front Immunol* 2018;**9**:2405.

Wagner TM, Romero-Saavedra F, Laverde D *et al.* Enterococcal membrane vesicles as vaccine candidates. *Int J Mol Sci* 2023;**24**:16051.

Weiner LM, Webb AK, Limbago B *et al.* Antimicrobial-resistant pathogens associated with healthcare-associated infections: summary of data reported to the National Healthcare Safety Network at the Centers for Disease Control and Prevention, 2011-2014. *Infect Control Hosp Epidemiol* 2016;**37**:1288–301.

Werneburg GT. Catheter-associated urinary tract infections: current challenges and future prospects. *Res Rep Urol* 2022;**14**:109–33.

Zawada JF, Yin G, Steiner AR *et al.* Microscale to manufacturing scale-up of cell-free cytokine production–a new approach for shortening protein production development timelines. *Biotechnol Bioeng* 2011;**108**:1570–8.

Received 4 April 2024; **revised** 13 September 2024; **accepted** 2 October 2024